



PII S0016-7037(00)00350-1

Theoretical studies of ^{238}U - ^{230}Th - ^{226}Ra and ^{235}U - ^{231}Pa disequilibria in young lavas produced by mantle melting

HAIBO ZOU^{1,2,*} and ALAN ZINDLER²

¹Department of Earth and Space Sciences, University of California at Los Angeles, Los Angeles, CA 90095, USA

²Division of Geochemistry, National High Magnetic Field Laboratory and Department of Geological Sciences, Florida State University, Tallahassee, FL 32306, USA

(Received June 23, 1999; accepted in revised form February 11, 2000)

Abstract—This paper provides ready-to-use equations to describe variations in uranium-series (U-series) disequilibrium as a function of elemental distribution coefficients, melting porosity, melting rate, and melting time. The effects of these melting parameters on U-series disequilibria are quantitatively evaluated in both an absolute and relative sense. The importance of net elemental fractionation and ingrowth of daughter nuclides are also described and compared in terms of their relative contributions to total U-series disequilibrium. In addition, we compare the production of U-series disequilibrium during mantle melting to trace element fractionations produced by melting in a similar context. Trace element fractionations depend externally on the degree to which a source is melted, whereas U-series disequilibrium depends upon both the degree and rate of melting. In contrast to previous models, our approach to modeling U-series disequilibrium during dynamic melting collapses simply to a description of trace element behavior during dynamic melting when the appropriate decay terms are omitted. Our formulation shows that extremely small degrees of melting, sometimes called upon to explain observed extents of U-series disequilibrium, are not always required. Copyright © 2000 Elsevier Science Ltd

1. INTRODUCTION

^{238}U decays to stable ^{206}Pb , and ^{235}U decays to stable ^{207}Pb via two different chains of short-lived intermediate nuclides with a wide range of half-lives. Among these intermediate nuclides, ^{230}Th and ^{226}Ra from ^{238}U and ^{231}Pa from ^{235}U are of particular importance to the study of melt generation and extraction. The half-lives of ^{230}Th , ^{226}Ra and ^{231}Pa are 75,200 y, 1600 y, and 32,800 y, respectively, and bracket the time scales of melt generation and extraction. In addition, mantle sources can be safely assumed to be in radioactive equilibrium regardless of their chemical compositions, which avoids uncertainties in initial source composition before melting. Therefore, observed secular disequilibria among the uranium-series (U-series) nuclides in young lavas may provide important information on mantle melting processes and the time scales of melt generation (e.g., Allègre and Condomines, 1982; Rubin and Macdougall, 1988; Lundstrom et al., 1995; Bourdon et al., 1996). Quantitative models that relate the extents of U-series disequilibria to the melting process have been proposed by McKenzie (1985), Williams and Gill (1989), Spiegelman and Elliott (1993), Qin (1993), Iwamori (1994), and Richardson and McKenzie (1994). Previous modeling of U-series disequilibria during dynamic partial melting with instant melt extraction has expressed ($^{230}\text{Th}/^{238}\text{U}$) and ($^{226}\text{Ra}/^{230}\text{Th}$) in young magmas as functions of porosity (ϕ) and melting rate (\dot{M}) by assuming that the melting time, T , approaches infinity (McKenzie, 1985; Beattie, 1993a; Chabaux and Allègre, 1994). Williams and Gill (1989) further incorporated melting time into the expressions for (^{230}Th) and (^{226}Ra). However, when setting all decay constants to be zero, their equations (Eqns. A16, A17, and A20) do

not collapse to the description of trace element behavior in the extracted melt during dynamic melting. The principal aims of this paper are:

1. to obtain three general ready-to-use equations, describing the variations of ($^{230}\text{Th}/^{238}\text{U}$), ($^{226}\text{Ra}/^{230}\text{Th}$), and ($^{231}\text{Pa}/^{235}\text{U}$) in recent magmas, as functions of ϕ , \dot{M} , and T ;
2. to quantitatively investigate the effect of ϕ , \dot{M} , T and the distribution coefficients of U and Th on U-series disequilibria in young lavas; and
3. to quantify the relative contributions from net elemental fractionation and ingrowth of daughter nuclides to the total U-series disequilibria.

2. DERIVATION OF EQUATIONS

If solid and melt are in equilibrium during partial melting, the conservation law which is concerned with the concentration of a radioactive and radiogenic nuclide in the solid and melt is given by McKenzie (1985) as the following differential equation

$$[\rho_f \phi + \rho_s(1 - \phi)D_d] \frac{\partial C_f^d}{\partial t} = (D_d - 1)C_f^d \dot{M} - \lambda_d[\rho_f \phi + \rho_s(1 - \phi)D_d]C_f^d + \lambda_p[\rho_f \phi + \rho_s(1 - \phi)D_p]C_p^d \quad (1)$$

The first term on the right-hand side is the melting term; the second term on the right-hand side is the radioactive decay of the nuclide; and the last term on the right-hand side represents the radiogenic production by the parent of the nuclide. C_f^d and C_p^d are the concentrations of the nuclide and its parent in the melt, respectively. D_d and D_p are the distribution coefficients of the nuclide and its parent, respectively. ρ_s is the density of the solid (3300 kg/m³), ρ_f is the density of the melt (2800 kg/m³), ϕ is the volume porosity of the mantle, \dot{M} is the melting rate

*Author to whom correspondence should be addressed (hzou@ess.ucla.edu).

(kg/m³/y), λ_d and λ_p are the decay constants of the nuclide and its parent, respectively. The solid concentration of the nuclide C_s^d is related to C_f^d by $C_s^d = D_d C_f^d$ and the solid concentration of its parent C_s^p is related to C_f^p by $C_s^p = D_p C_f^p$.

Eqn. 1 can be scaled as

$$\frac{\partial(C_f^d)}{\partial t} = -(\alpha_d + \lambda_d)(C_f^d) + \lambda_d \frac{F_d}{F_p}(C_f^p) \quad (2)$$

where

$$\alpha_d(\phi, \dot{M}) = \frac{(1 - D_d)\dot{M}}{\rho_f \phi + D_d \rho_s (1 - \phi)} \quad (3)$$

$$F_i(\phi) = \frac{\rho_f \phi}{D_i \rho_s (1 - \phi) + \rho_f \phi} \quad (4)$$

and (C_f^d) and (C_f^p) are the activities [defined as the product of its concentration C and decay constant λ , and denoted by parentheses, $(C_f^d) = \lambda_d C_f^d$, and $(C_f^p) = \lambda_p C_f^p$] of the nuclide and the parent nuclide in the melt, respectively. α_d is the melting parameter for the nuclide and has the same dimension (y⁻¹) as the radioactive parameter λ . The subscript i in Eqn. 4 may represent a daughter or its parent.

Eqn. 2 can be used to model the uranium decay series (U-series) nuclides in the residual melt during dynamic partial melting:

$$\frac{d(^{238}U)_f}{dt} = -(\alpha_U + \lambda_{238})(^{238}U)_f \quad (5)$$

$$\frac{d(^{230}Th)_f}{dt} = -(\alpha_{Th} + \lambda_{230})(^{230}Th)_f + \lambda_{230} \frac{F_{Th}}{F_U} (^{238}U)_f \quad (6)$$

$$\frac{d(^{226}Ra)_f}{dt} = -(\alpha_{Ra} + \lambda_{226})(^{226}Ra)_f + \lambda_{226} \frac{F_{Ra}}{F_{Th}} (^{230}Th)_f \quad (7)$$

$(^{238}U)_f$, $(^{230}Th)_f$, and $(^{226}Ra)_f$ are the activities of ²³⁸U, ²³⁰Th, and ²²⁶Ra in the residual melt. Eqn. 5 is different from Eqn. 6 and Eqn. 7 because ²³⁸U, unlike ²³⁰Th or ²²⁶Ra, has no parent. For dynamic melting, the melting rate (\dot{M}) is constant in the upwelling material and the melt fraction (ϕ) in equilibrium with the matrix remains constant because additional melt is drained into a melt channel (the details of the model are shown in Figure 3 in McKenzie, 1985; Figure 3 in Elliott, 1997; and Figures 1 and 3 in Zou, 1998). In this case, both α and F are independent of time (see Eqns. 3 and 4) and the system of differential Eqns 5–7 has explicit solutions:

$$(^{238}U)_f = (^{238}U)_f^0 \exp[-(\alpha_U + \lambda_{238})t] \quad (8)$$

$$\begin{aligned} (^{230}Th)_f &= (^{230}Th)_f^0 \exp[-(\alpha_{Th} + \lambda_{230})t] \\ &+ \frac{\lambda_{230}}{\alpha_{Th} + \lambda_{230} - \alpha_U - \lambda_{238}} \frac{F_{Th}}{F_U} (^{238}U)_f^0 \{ \exp[-(\alpha_U + \lambda_{238})t] \\ &- \exp[-(\alpha_{Th} + \lambda_{230})t] \} \quad (9) \end{aligned}$$

$$\begin{aligned} (^{226}Ra)_f &= (^{226}Ra)_f^0 \exp[-(\alpha_{Ra} + \lambda_{226})t] \\ &+ \frac{\lambda_{226}}{\alpha_{Ra} + \lambda_{226} - \alpha_{Th} - \lambda_{230}} \frac{F_{Ra}}{F_{Th}} (^{230}Th)_f^0 \\ &\{ \exp[-(\alpha_{Th} + \lambda_{230})t] - \exp[-(\alpha_{Ra} + \lambda_{226})t] \} \\ &+ \frac{\lambda_{230}\lambda_{226}}{\alpha_{Th} + \lambda_{230} - \alpha_U - \lambda_{238}} \frac{F_{Ra}}{F_U} (^{238}U)_f^0 \\ &\left\{ \frac{\exp[-(\alpha_U + \lambda_{238})t] - \exp[-(\alpha_{Ra} + \lambda_{226})t]}{\alpha_{Ra} + \lambda_{226} - \alpha_U - \lambda_{238}} \right. \\ &\left. - \frac{\exp[-(\alpha_{Th} + \lambda_{230})t] - \exp[-(\alpha_{Ra} + \lambda_{226})t]}{\alpha_{Ra} + \lambda_{226} - \alpha_{Th} - \lambda_{230}} \right\} \quad (10) \end{aligned}$$

The solutions for the residual melt are the same as those obtained by McKenzie (1985) for $(^{238}U)_f$ and $(^{230}Th)_f$, and Williams and Gill (1989) for $(^{226}Ra)_f$ except that the decay constant of ²³⁸U (λ_{238}) is included here. As basalts are considered as extracted melts, the next important step is to derive the equations for the extracted melt from the solutions for the residual melt. The real difference of this study from previous ones starts from this step. The ²³⁸U, ²³⁰Th and ²²⁶Ra activities of the extracted melt produced by dynamic melting will be average values of the residual melt. An average activity of a nuclide in the extracted melt, (C) , can be approximately obtained by averaging relative to melting time (T) (e.g., McKenzie, 1985; Chabaux and Allègre, 1994),

$$(C) = \frac{1}{T} \int_0^T (C_f(t)) dt \quad (11)$$

The accurate activity of the nuclide in the extracted melt will be the average values of these functions for the residual melt with respect to X , the mass fraction of extracted melt relative to the initial amount (Williams and Gill, 1989)

$$(C) = \frac{1}{X} \int_0^X (C_f(X)) dX = \frac{1}{X} \int_0^T \left(C_f(t) \frac{dX}{dt} \right) dt \quad (12)$$

Another key for the derivation of the equation for (C) is to accurately express X as a function of ϕ , \dot{M} , and t in order to obtain dX/dt in Eqn. 12. X is related to \dot{M}_e (the melt extraction rate), ϕ , and t by the following relationship (Zou, 1998)

$$X = 1 - \exp\left[-\frac{\dot{M}_e}{\rho_f \phi + \rho_s (1 - \phi)} t\right] \quad (13)$$

where \dot{M}_e is related to the melting rate \dot{M} by (Zou, 1998)

$$\frac{\dot{M}}{\dot{M}_e} = \frac{\rho_s (1 - \phi)}{\rho_f \phi + \rho_s (1 - \phi)} \quad (14)$$

Combining Eqn. 13 with Eqn. 14, we obtain

$$X(\phi, \dot{M}, t) = 1 - \exp\left[-\frac{\dot{M}}{\rho_s (1 - \phi)} t\right] \quad (15)$$

Consequently,

$$\frac{dX}{dt} = \frac{\dot{M}}{\rho_s(1-\phi)} \exp\left[-\frac{\dot{M}}{\rho_s(1-\phi)}t\right] \quad (16)$$

Combining Eqn. 12, Eqn. 16 with Eqns. 8–10, respectively, we have

$$\frac{{}^{(238U)}X}{\theta} = \frac{{}^{(238U)}_f^0}{\alpha_U + \lambda_{238} + \theta} \{1 - \exp[-(\alpha_U + \lambda_{238} + \theta)T]\} \quad (17)$$

$$\begin{aligned} \frac{{}^{(230Th)}X}{\theta} &= \frac{\lambda_{230}}{\alpha_{Th} + \lambda_{230} - \alpha_U - \lambda_{238}} \frac{1}{\alpha_U + \lambda_{238} + \theta} \frac{F_{Th}}{F_U} {}^{(238U)}_f^0 \\ &\quad \{1 - \exp[-(\alpha_U + \lambda_{238} + \theta)T]\} \\ &+ \frac{(\alpha_{Th} + \lambda_{230} - \alpha_U - \lambda_{238})({}^{(230Th)}_f^0) - \lambda_{230}\left(\frac{F_{Th}}{F_U}\right)({}^{(238U)}_f^0)}{(\alpha_{Th} + \lambda_{230} + \theta)(\alpha_{Th} + \lambda_{230} - \alpha_U - \lambda_{238})} \\ &\quad \{1 - \exp[-(\alpha_{Th} + \lambda_{230} + \theta)T]\} \quad (18) \end{aligned}$$

$$\begin{aligned} \frac{{}^{(226Ra)}X}{\theta} &= \frac{\lambda_{230}\lambda_{226}}{(\alpha_{Th} + \lambda_{230} - \alpha_U - \lambda_{238})(\alpha_{Ra} + \lambda_{226} - \alpha_U - \lambda_{238})} \\ &\quad \frac{F_{Ra}}{F_U} {}^{(238U)}_f^0 \frac{1 - \exp[-(\alpha_U + \lambda_{238} + \theta)T]}{\alpha_U + \lambda_{238} + \theta} \\ &\quad + \frac{1}{\alpha_{Ra} + \lambda_{226} - \alpha_{Th} - \lambda_{230}} \\ &\quad \times \left[\frac{\lambda_{226} \frac{F_{Ra}}{F_{Th}} ({}^{(230Th)}_f^0) - \lambda_{230}\lambda_{226} \frac{F_{Ra}}{F_U} ({}^{(238U)}_f^0)}{\alpha_{Th} + \lambda_{230} - \alpha_U - \lambda_{238}} \right] \\ &\quad \times \frac{1 - \exp[-(\alpha_{Th} + \lambda_{230} + \theta)T]}{\alpha_{Th} + \lambda_{230} + \theta} + \\ &\quad \left[\frac{{}^{(226Ra)}_f^0 - \frac{\lambda_{226}}{\alpha_{Ra} + \lambda_{226} - \alpha_{Th} - \lambda_{230}} \frac{F_{Ra}}{F_{Th}} ({}^{(230Th)}_f^0)}{\lambda_{230}\lambda_{226}} \frac{F_{Ra}}{F_U} ({}^{(238U)}_f^0) \right] \end{aligned}$$

$${}^{(226Ra)} = \frac{{}^{(226Ra)}_f^0}{X} \frac{\theta}{\alpha_U + \lambda_{238} + \theta} \left\{ c_3 \{1 - \exp[-(\alpha_U + \lambda_{238} + \theta)T]\} + c_4 \{1 - \exp[-(\alpha_{Th} + \lambda_{230} + \theta)T]\} + c_5 \{1 - \exp[-(\alpha_{Ra} + \lambda_{226} + \theta)T]\} \right\} \quad (26)$$

where

$$\begin{aligned} c_1 &= \frac{\lambda_{230}}{\alpha_{Th} + \lambda_{230} - \alpha_U - \lambda_{238}} \\ c_2 &= \frac{(\alpha_U + \lambda_{238} + \theta)(\alpha_{Th} - \alpha_U - \lambda_{238})}{(\alpha_{Th} + \lambda_{230} + \theta)(\alpha_{Th} + \lambda_{230} - \alpha_U - \lambda_{238})} \\ c_3 &= \frac{\lambda_{230}\lambda_{226}}{(\alpha_{Th} + \lambda_{230} - \alpha_U - \lambda_{238})(\alpha_{Ra} + \lambda_{226} - \alpha_U - \lambda_{238})} \\ c_4 &= \frac{\lambda_{226}(\alpha_U + \lambda_{238} + \theta)}{(\alpha_{Th} + \lambda_{230} + \theta)(\alpha_{Ra} + \lambda_{226} - \alpha_{Th} - \lambda_{230})} \\ &\quad \times \frac{\alpha_{Th} - \alpha_U - \lambda_{238}}{\alpha_{Th} + \lambda_{230} - \alpha_U - \lambda_{238}} \\ c_5 &= \frac{\alpha_U + \lambda_{238} + \theta}{(\alpha_{Ra} + \lambda_{226} + \theta)(\alpha_{Ra} + \lambda_{226} - \alpha_{Th} - \lambda_{230})} \\ &\quad \times \left(\alpha_{Ra} - \alpha_{Th} - \lambda_{230} + \frac{\lambda_{230}\lambda_{226}}{\alpha_{Ra} + \lambda_{226} - \alpha_U - \lambda_{238}} \right) \end{aligned}$$

$$\frac{1 - \exp[-(\alpha_{Ra} + \lambda_{226} + \theta)T]}{\alpha_{Ra} + \lambda_{226} + \theta} \quad (19)$$

where

$$\theta(\phi, \dot{M}) = \frac{\dot{M}}{\rho_s(1-\phi)} \quad (20)$$

$({}^{(238U)}_f^0)$, $({}^{(230Th)}_f^0)$, and $({}^{(226Ra)}_f^0)$ are the initial activities of ${}^{238}\text{U}$, ${}^{230}\text{Th}$, and ${}^{226}\text{Ra}$ in the first drop of the extracted melt. It should be emphasized that, when setting all the decay constants to be zero, Eqns. 17–19 reduce to Eqn. 14 in Zou (1998) which describes trace element concentrations in the extracted melt in the context of modal dynamic melting

$$C = \frac{1}{X} C_o \{1 - (1 - X)^{[\rho_f \phi + \rho_s(1-\phi)]/[\rho_f \phi + \rho_s(1-\phi)D]}\} \quad (21)$$

The final step is to obtain ready-to-use equations for $({}^{(230Th)}/{}^{(238U)})$ and $({}^{(226Ra)}/{}^{(230Th)})$. To do so, we need to know the relationship among the initial conditions $({}^{(238U)}_f^0)$, $({}^{(230Th)}_f^0)$, and $({}^{(226Ra)}_f^0)$ in Eqns. 17–19 so as to eventually eliminate these initial conditions from the expressions for $({}^{(230Th)}/{}^{(238U)})$ and $({}^{(226Ra)}/{}^{(230Th)})$. The relationship between $({}^{(230Th)}_f^0)$ and $({}^{(238U)}_f^0)$ has been given by O'Nions and McKenzie (1993) as

$$({}^{(230Th)}_f^0)/({}^{(238U)}_f^0) = F_{Th}/F_U \quad (22)$$

Similarly, we have

$$({}^{(226Ra)}_f^0)/({}^{(230Th)}_f^0) = F_{Ra}/F_{Th} \quad (23)$$

$$({}^{(231Pa)}_f^0)/({}^{(235U)}_f^0) = F_{Pa}/F_U \quad (24)$$

Substituting Eqns. 22–24 into Eqns. 18 and 19, we obtain

$$({}^{(230Th)}) = \frac{{}^{(230Th)}_f^0}{X} \frac{\theta}{\alpha_U + \lambda_{238} + \theta} \{c_1 \{1 - \exp[-(\alpha_U + \lambda_{238} + \theta)T]\} + c_2 \{1 - \exp[-(\alpha_{Th} + \lambda_{230} + \theta)T]\} \} \quad (25)$$

Therefore, ($^{230}\text{Th}/^{238}\text{U}$) and ($^{226}\text{Ra}/^{230}\text{Th}$) in the extracted melt are given by

$$\frac{(^{230}\text{Th})}{(^{238}\text{U})}(\phi, \dot{M}, T) = \frac{F_{Th}}{F_U} \left\{ c_1 + c_2 \frac{1 - \exp[-(\alpha_{Th} + \lambda_{230} + \theta)T]}{1 - \exp[-(\alpha_U + \lambda_{238} + \theta)T]} \right\} \quad (27)$$

$$\frac{(^{226}\text{Ra})}{(^{230}\text{Th})}(\phi, \dot{M}, T) = \frac{F_{Ra}}{F_{Th}} \frac{\left\{ c_3 \{1 - \exp[-(\alpha_U + \lambda_{238} + \theta)T]\} + c_4 \{1 - \exp[-(\alpha_{Th} + \lambda_{230} + \theta)T]\} \right\}}{c_1 \{1 - \exp[-(\alpha_U + \lambda_{238} + \theta)T]\} + c_2 \{1 - \exp[-(\alpha_{Th} + \lambda_{230} + \theta)T]\}} \quad (28)$$

The system of differential equations 5 and 6 for ^{238}U - ^{230}Th systematics (rather than that of Eqns. 6 and 7 for ^{230}Th - ^{226}Ra systematics) is also suitable for ^{235}U - ^{231}Pa systematics, therefore,

$$\frac{(^{231}\text{Pa})}{(^{235}\text{U})}(\phi, \dot{M}, T) = \frac{F_{Pa}}{F_U} \left\{ c_6 + c_7 \frac{1 - \exp[-(\alpha_{Pa} + \lambda_{231} + \theta)T]}{1 - \exp[-(\alpha_U + \lambda_{235} + \theta)T]} \right\} \quad (29)$$

where

$$c_6 = \frac{\lambda_{231}}{\alpha_{Pa} + \lambda_{231} - \alpha_U - \lambda_{235}}$$

$$c_7 = \frac{(\alpha_U + \lambda_{235} + \theta)(\alpha_{Pa} - \alpha_U - \lambda_{235})}{(\alpha_{Pa} + \lambda_{231} + \theta)(\alpha_{Pa} + \lambda_{231} - \alpha_U - \lambda_{235})}$$

λ_{235} and λ_{231} are decay constants of ^{235}U and ^{231}Pa , respectively. Note that c_1 to c_7 are functions of ϕ and \dot{M} only and they are dimensionless because λ , ϕ , and α have the same dimension. Eqns. 27–29 are the general equations that will be used for modeling here.

Two limit cases (when $T \rightarrow 0$ or $T \rightarrow \infty$) for ($^{230}\text{Th}/^{238}\text{U}$), ($^{226}\text{Ra}/^{230}\text{Th}$) and ($^{231}\text{Pa}/^{235}\text{U}$) can be obtained from the general Eqns. 27–29. When $T \rightarrow 0$, Eqns. 27–29 become Eqns. 22–24, which are the initial conditions, respectively. On the other hand, when $T \rightarrow \infty$, Eqns. 27–29 reduce to

$$\frac{(^{230}\text{Th})_\infty}{(^{238}\text{U})_\infty}(\phi, \dot{M}) = \frac{F_{Th}}{F_U} \left\{ \frac{\alpha_U + \lambda_{238} + \lambda_{230} + \theta}{\alpha_{Th} + \lambda_{230} + \theta} \right\} \quad (30)$$

$$\frac{(^{226}\text{Ra})_\infty}{(^{230}\text{Th})_\infty}(\phi, \dot{M}) = \frac{F_{Ra}}{F_{Th}} \frac{\alpha_{Th} + \lambda_{226} + \theta}{\alpha_{Ra} + \lambda_{226} + \theta} \times \left[1 + \frac{\lambda_{230}(\alpha_U + \lambda_{238} - \alpha_{Th})}{(\alpha_{Th} + \lambda_{226} + \theta)(\alpha_U + \lambda_{238} + \lambda_{230} + \theta)} \right] \quad (31)$$

$$\frac{(^{231}\text{Pa})_\infty}{(^{235}\text{U})_\infty}(\phi, \dot{M}) = \frac{F_{Pa}}{F_U} \left\{ \frac{\alpha_U + \lambda_{235} + \lambda_{231} + \theta}{\alpha_{Pa} + \lambda_{231} + \theta} \right\} \quad (32)$$

If we set θ , λ_{235} , and λ_{238} to be zero, Eqn. 30 reduces to Eqn. 25 in McKenzie (1985) and Eqn. 31 reduces to the last equation in Appendix 2 of Chabaux and Allègre (1994).

3. FORWARD MODELING RESULTS

The distribution coefficients of the parent and daughter nuclides are very important in U-series disequilibria. If the parent has a higher distribution coefficient than the daughter, its extraction from the matrix is retarded and the daughter/parent

activity ratio in the melt can be greater than 1. Experiments (Beattie, 1993a; Beattie, 1993b; LaTourrette et al., 1992; LaTourrette et al., 1993; Lundstrom et al., 1994; Hauri et al., 1994; Salters and Longhi, 1999) have shown that $D_U > D_{Th}$ for garnet peridotites but $D_U < D_{Th}$ for spinel peridotites at low pressures. Due to experimental difficulties, D_{Ra} and D_{Pa} are not directly known but are inferred to be very small (e.g., Pickett and Murrell, 1997; Wood et al., 1999). Therefore, it is reasonable to assume $D_{Th} > D_{Ra}$ and $D_U > D_{Pa}$ for both garnet peridotites and spinel peridotites.

If melting takes place in the garnet stability field ($D_U > D_{Th} > D_{Ra}$ and $D_U > D_{Pa}$), then $\alpha_U < \alpha_{Th} < \alpha_{Ra}$ and $\alpha_U < \alpha_{Pa}$ (Eqn. 3). The left-hand sides of Eqns. 27–29 are all decreasing functions of melting time (Fig. 1). At low melting times, there is greater disequilibrium due to a strong component of net elemental fractionation of parent and daughter at low degrees of melting. The disequilibrium becomes smaller at high melting times as a result of small net elemental fractionation, and the disequilibrium is dominated by the component of in-growth of daughter nuclides. The form of the curves in Figure 1 reflects the transition from the former to the later with increasing time. In addition, small porosity and slow melting rate favor high ($^{230}\text{Th}/^{238}\text{U}$), ($^{226}\text{Ra}/^{230}\text{Th}$) and ($^{231}\text{Pa}/^{235}\text{U}$) in magmas (Fig. 1A–F), which is consistent with previous assessment by McKenzie (1985) about the effect of melting rate and porosity on ($^{230}\text{Th}/^{238}\text{U}$). However, the sensitivity of the daughter/parent activity ratio to the variations of ϕ , \dot{M} , and T is different for the above three activity ratios. Both ($^{230}\text{Th}/^{238}\text{U}$) and ($^{231}\text{Pa}/^{235}\text{U}$) are sensitive to the variations of ϕ , \dot{M} , and T . In contrast, ($^{226}\text{Ra}/^{230}\text{Th}$) is sensitive to ϕ but very insensitive to \dot{M} and, in particular, T (Figs. 1B and 1E).

If melting takes place at low pressures in the spinel stability field ($D_U < D_{Th}$, $D_{Th} > D_{Ra}$, and $D_U > D_{Pa}$), then $\alpha_U > \alpha_{Th}$, $\alpha_{Th} < \alpha_{Ra}$, and $\alpha_U < \alpha_{Pa}$. Eqn. 27 is an increasing function of melting time while Eqns. 28–29 are still decreasing functions of melting time (Fig. 2A–F). In contrast to the case for garnet peridotite mantle, large porosity, fast melting rate and long melting time in the spinel peridotite source actually favor the generation of high (but less than 1) ($^{230}\text{Th}/^{238}\text{U}$). As for ($^{226}\text{Ra}/^{230}\text{Th}$) and ($^{231}\text{Pa}/^{235}\text{U}$), they show the similar trends as those for garnet peridotites. ($^{226}\text{Ra}/^{230}\text{Th}$) is still only sensitive to the variation of porosity while ($^{231}\text{Pa}/^{235}\text{U}$) is sensitive to the variation of ϕ , \dot{M} , and T . And significant ^{226}Ra excess generally indicates that the melting porosity is small (<1%). The great dependence of ($^{226}\text{Ra}/^{230}\text{Th}$) on melting porosity has been discovered by Beattie (1993) from a dynamic melting model and by Spiegelman and Elliott (1993) from a steady-state reactive porous flow model.

Figures 1 and 2 show that the relative magnitude of the

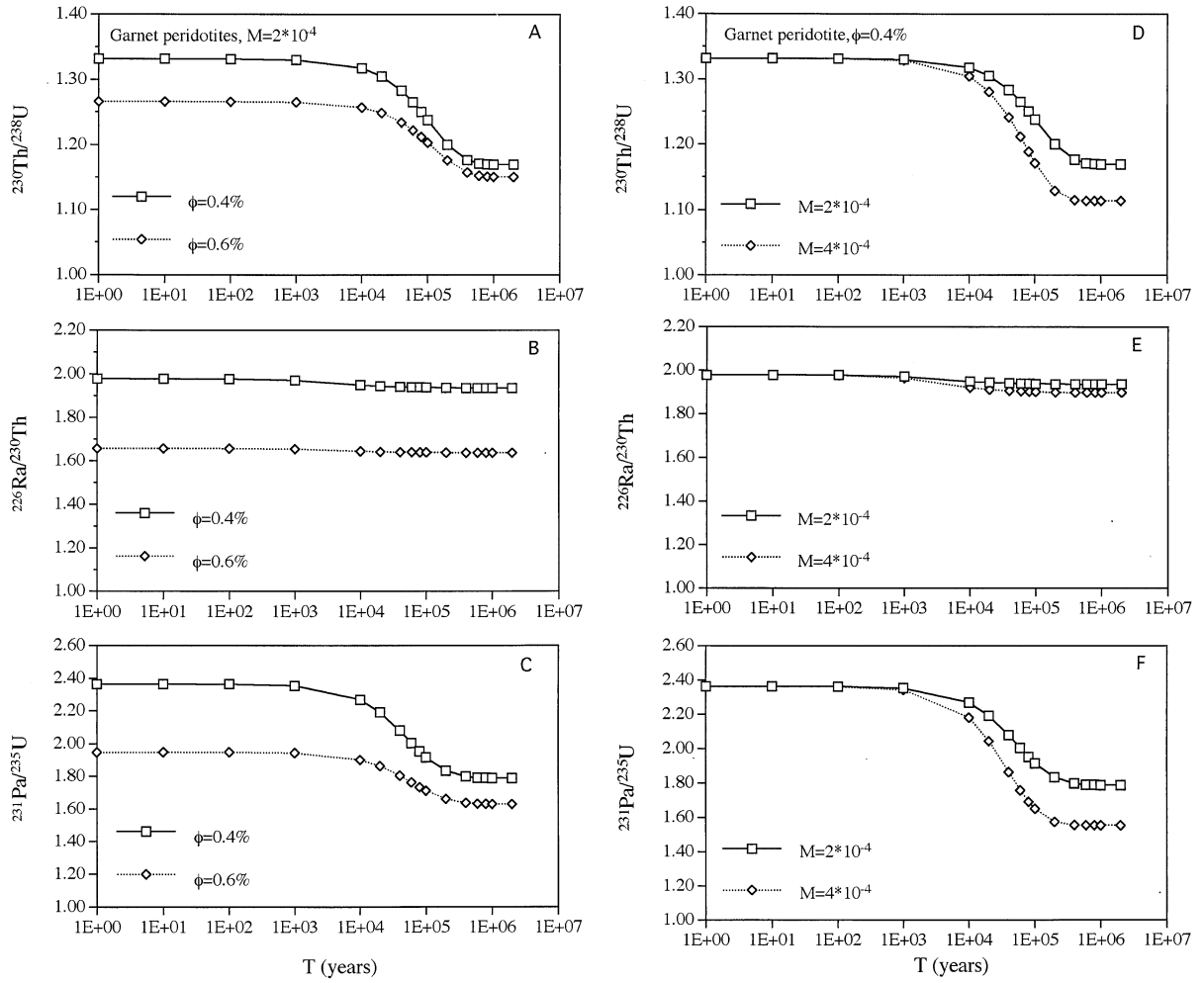


Fig. 1. (A–C) variations of ($^{230}\text{Th}/^{238}\text{U}$), ($^{226}\text{Ra}/^{230}\text{Th}$), and ($^{231}\text{Pa}/^{235}\text{U}$) as functions of T (in years) and ϕ at a constant \dot{M} ($= 2 \times 10^{-4}$ kg/m³/year) for a garnet peridotite source. (D–F) variations of ($^{230}\text{Th}/^{238}\text{U}$), ($^{226}\text{Ra}/^{230}\text{Th}$), and ($^{231}\text{Pa}/^{235}\text{U}$) as functions of T and \dot{M} for a constant ϕ ($= 0.4\%$) for a garnet peridotite source. Distribution coefficients: $D_{\text{Th}}(\text{gt}) = 0.019$, $D_{\text{U}}(\text{gt}) = 0.041$, $D_{\text{Th}}(\text{opx}) = 0.0002$, $D_{\text{U}}(\text{opx}) = 0.0005$ (Salters and Longhi, 1999), $D_{\text{Th}}(\text{cpx}) = 0.015$, $D_{\text{U}}(\text{cpx}) = 0.010$ (Lundstrom et al., 1994), $D_{\text{Th}}(\text{ol}) = D_{\text{U}}(\text{ol}) = D_{\text{Th}}(\text{sp}) = D_{\text{U}}(\text{sp}) = 0.00001$ (assumed). The mineral compositions for garnet peridotites are gt 12%, cpx 8%, ol 59%, opx 21% (Beattie, 1993). The calculated bulk distribution coefficients are $D_{\text{Th}} = 0.00353$ and $D_{\text{U}} = 0.00583$ for garnet peridotites. The bulk distribution coefficients for Ra and Pa are assumed as $D_{\text{Ra}} = 0.0001$ and $D_{\text{Pa}} = 0.0005$ for garnet peridotites.

daughter and parent distribution coefficients actually determines whether a correlation is positive or negative between the daughter/parent activity ratio and any one of the three parameters (ϕ , \dot{M} , and T). If the distribution coefficient of the daughter is smaller than that of its parent, a negative correlation is shown between the daughter/parent activity ratio and any of the above three parameters. For example, if $D_{\text{Pa}} < D_{\text{U}}$, then short melting time, small porosity, and slow melting rate favor the generation of high ($^{231}\text{Pa}/^{235}\text{U}$) values, and vice versa.

Eqn. 31 for ($^{226}\text{Ra}/^{230}\text{Th}$)_∞ and Eqn. 32 for ($^{231}\text{Pa}/^{235}\text{U}$)_∞ give the minimum values for ($^{226}\text{Ra}/^{230}\text{Th}$) and ($^{231}\text{Pa}/^{235}\text{U}$), respectively. As for Eqn. 30 for ($^{230}\text{Th}/^{238}\text{U}$)_∞, it gives the minimum values if melting takes place in a garnet peridotite source and a maximum value for melting of a spinel peridotite source. In addition, Eqn. 31 for ($^{226}\text{Ra}/^{230}\text{Th}$)_∞ in general gives a value that is very close to the exact solution from Eqn. 28 no matter how long the melting time is. Eqns. 30 and 32 give

approximately correct daughter/parent activity ratios when the melting time is long or when the fraction of the extracted melt is high. According to Figs. 1 and 2, when T is close to about 10^6 years, the values calculated from Eqns. 30 and 32 would be very close to the exact solution calculated from Eqns. 27 and 29, respectively. The characteristic melting time (T_c) after which Eqns. 30 and 32 return values that are very close to the exact solution depends on the choices of distribution coefficients, the melting rate, and the porosity. Steady state is not necessarily at infinite melting times and can be reached at a characteristic time.

The values of ($^{230}\text{Th}/^{238}\text{U}$)_∞ and ($^{226}\text{Ra}/^{230}\text{Th}$)_∞ have been frequently used to estimate melting porosity and melting rate (Cohen and O’Nions, 1993; Hemond et al., 1994; Chabaux and Allègre, 1994). This estimate from the simplified equation is applicable when the melting time is long ($T > T_c$). In comparison, the pair of ($^{231}\text{Pa}/^{235}\text{U}$)_∞ and ($^{226}\text{Ra}/^{230}\text{Th}$)_∞ have seldom

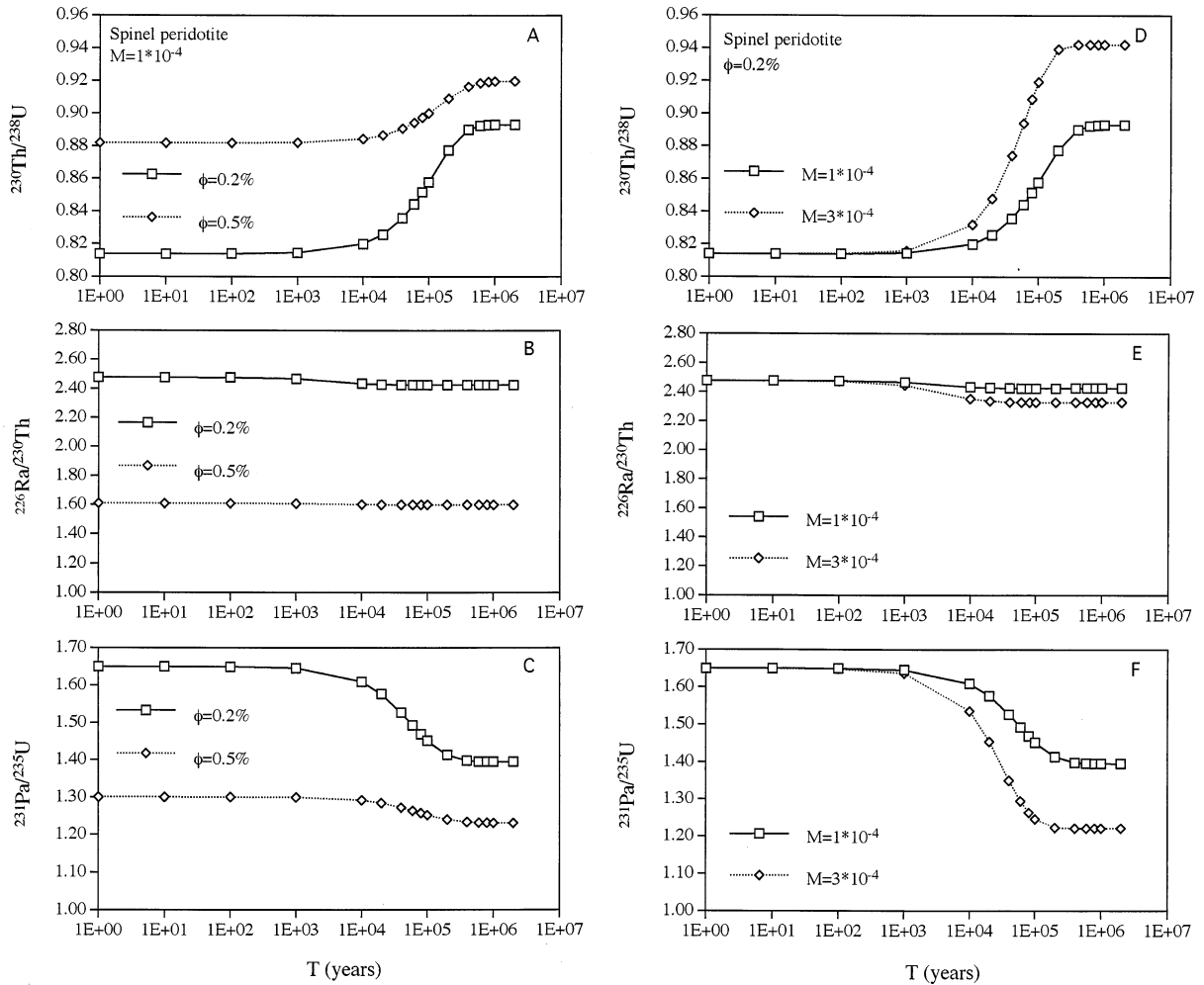


Fig. 2. (A–C) Variations of ($^{230}\text{Th}/^{238}\text{U}$), ($^{226}\text{Ra}/^{230}\text{Th}$), and ($^{231}\text{Pa}/^{235}\text{U}$) as functions of T (in years) and ϕ for a constant \dot{M} ($= 1 \times 10^{-4}$ kg/m³/year) for a spinel peridotite source. (D–F) variations of ($^{230}\text{Th}/^{238}\text{U}$), ($^{226}\text{Ra}/^{230}\text{Th}$), and ($^{231}\text{Pa}/^{235}\text{U}$) as functions of T and \dot{M} for a constant ϕ ($= 0.2\%$) for a spinel peridotite source. The mineral/melt distribution coefficients are the same as those in Figure 1. The mineral compositions for spinel peridotites are cpx 18%, ol 55%, opx 25%, sp 2% (Johnson et al., 1990). The calculated bulk distribution coefficients are $D_{\text{Th}} = 0.00276$ and $D_{\text{U}} = 0.00193$ for spinel peridotites. The bulk distribution coefficients for Ra and Pa are assumed as $D_{\text{Ra}} = 0.0001$ and $D_{\text{Pa}} = 0.0005$ for spinel peridotites.

been used but have a potential advantage over the frequently used pair in that ($^{231}\text{Pa}/^{235}\text{U}$)_∞ is empirically less sensitive to the types of the source rocks (spinel peridotites or garnet peridotites) compared with ($^{230}\text{Th}/^{238}\text{U}$)_∞. The disadvantage of using ($^{231}\text{Pa}/^{235}\text{U}$)_∞ instead of ($^{230}\text{Th}/^{238}\text{U}$)_∞ at present lies in the paucity of the data for ($^{231}\text{Pa}/^{235}\text{U}$)_∞ in literature.

4. DISCUSSIONS AND SUMMARY

4.1. The Meanings of Melting Rate and Melt Extraction Rate

Although the melting rate \dot{M} plays an important role in U-series modeling, this parameter has not been rigorously defined in literature, which may have caused confusion in terms of understanding the melting process. Essentially, in order for Eqn. 1 to satisfy mass balance requirements for the dynamic melting model, \dot{M} should be defined as

$$\dot{M} = - \frac{1}{1-X} \frac{d[\rho_s(1-\phi)(1-X)]}{dt} \quad (33)$$

where $\rho_s(1-\theta)(1-X)$ is the mass of the residual solid per unit volume. Note that \dot{M} is a scaled parameter relative to the amount of the total residue ($1-X$) and has the dimension of mass per unit volume per unit time (e.g., kg/m³/year). If we divide \dot{M} by the density of the total residue, or, $\rho_f\phi + \rho_s(1-\phi)$, we can obtain a melting rate in per cent (of the total residue) per unit time as

$$\dot{M}' = - \frac{\rho_s(1-\phi)}{\rho_f\phi + \rho_s(1-\phi)} \frac{1}{1-X} \frac{d(1-X)}{dt} \quad (34)$$

\dot{M}' has a simpler dimension and is easy to understand as compared to \dot{M} . According to Eqn. 13, the rate of melt extraction (\dot{M}_e) is

$$\dot{M}_e = -\frac{1}{1-X} \frac{d\{\rho_f \phi + \rho_s(1-\phi)\}(1-X)}{dt} \quad (35)$$

where $[\rho_f \phi + \rho_s(1-\phi)](1-X)$ is the mass of total residue per unit volume and \dot{M}_e is also a scaled parameter relative to the amount of the total residue. The melt extraction rate in percent (of the total residue) per unit time can be obtained by dividing \dot{M}_e by the density of the total residue, or, $\rho_f \phi + \rho_s(1-\phi)$, we have

$$\dot{M}'_e = -\frac{1}{1-X} \frac{d(1-X)}{dt} \quad (36)$$

Comparison of Eqn. 33 with Eqn. 35 yields the relationship between \dot{M} and \dot{M}'_e

$$\frac{\dot{M}}{\dot{M}'_e} = \frac{\rho_s(1-\phi)}{\rho_f \phi + \rho_s(1-\phi)} \quad (37)$$

which is Eqn. 9 in Zou (1998) obtained from a different approach.

4.2. U-Series Modeling and the Degree of Partial Melting

Eqns. 27–29 express the variation of ($^{230}\text{Th}/^{238}\text{U}$), ($^{226}\text{Ra}/^{230}\text{Th}$), and ($^{231}\text{Pa}/^{235}\text{U}$) in the extracted melt as functions of ϕ , \dot{M} , and T (ϕ and \dot{M} are implicitly included in the melting parameter α). One might wonder why some commonly used parameters in trace element modeling, such as the degree of partial melting (f) or the fraction of extracted melt (X), are not included in these equations. This is due to the fact that F and X are also functions of ϕ , \dot{M} , and T for U-series modeling. The expression for X as a function of ϕ , \dot{M} , and T has been given by Eqn. 15. And f is related to X by (Zou, 1998),

$$f = \Phi + (1 - \Phi)X \quad (38)$$

where Φ is the mass porosity and is related to volume porosity (ϕ) by

$$\Phi = \frac{\rho_f \phi}{\rho_f \phi + \rho_s(1-\phi)} \quad (39)$$

For U-series modeling, we have five parameters in ϕ , \dot{M} , T , f and X . Since there are two equations (Eqns. 15 and 38) to relate these five parameters, we have three independent parameters. Theoretically, we can express ($^{230}\text{Th}/^{238}\text{U}$), ($^{226}\text{Ra}/^{230}\text{Th}$) and ($^{231}\text{Pa}/^{235}\text{U}$) as functions of any three of the above five parameters except for the combination of ϕ , f and X . For example, we may select ϕ , \dot{M} , and f as independent parameters. By combining Eqn. 38 with Eqn. 15, we have

$$f = \Phi + (1 - \Phi) \left\{ 1 - \exp \left[-\frac{\dot{M}T}{\rho_s(1-\phi)} \right] \right\} \quad (40)$$

or

$$T = \frac{\rho_s(1-\phi)}{\dot{M}} \ln \left(\frac{1-\Phi}{1-f} \right) \quad (41)$$

Substituting Eqn. 41 into Eqns. 27–29 results in the formula for ($^{230}\text{Th}/^{238}\text{U}$), ($^{226}\text{Ra}/^{230}\text{Th}$) and ($^{231}\text{Pa}/^{235}\text{U}$) as functions of ϕ , \dot{M} , and f . However, doing so will make these equations un-

essarily complex. In practice, the selection of ϕ , \dot{M} , and T leads to the simplest formula.

The physical significance of melting time has not been well handled before. Eqn. 41 is in fact the definition of melting time. It can be seen from Eqn. 41 that if $f = \Phi$, then $T = 0$; and if $f \rightarrow 1$, then $T \rightarrow \infty$. Accordingly, increasing melting time reflects increasing degrees of melting in these time-dependent melting calculations, and the scenario of infinite melting time corresponds to total melting. Therefore, melting time is the time period for the degree of partial melting increases from Φ to its final degree of melting at which the measured samples are produced. Physically, given a certain melting rate, the low melting times represent either simply a small amount of melting at low beta factors, or volcanism at the onset of complete rifting.

4.3. Activity Ratios in the Residual Melt When $f \leq \Phi$

Equations 27–29 describe the activity ratios in the extracted melt when $f > \Phi$. In this section we will discuss the behaviors of activity ratios when $f \leq \Phi$. Since there is no extracted melt when $f \leq \Phi$, we only study the behaviors in the residual melt. We will first describe the case when $f = \Phi$ (or the initial conditions) and then the case when $f < \Phi$. According to Eqn. 4, we have

$$F_{\text{Th}}/F_{\text{U}} = \frac{D_{\text{U}} \rho_s(1-\phi) + \rho_f \phi}{D_{\text{Th}} \rho_s(1-\phi) + \rho_f \phi} \quad (42)$$

Since the effective distribution coefficients for U and Th are

$$D_{\text{U}}^{\text{eff}} = \Phi + (1 - \Phi)D_{\text{U}} \quad (43)$$

$$D_{\text{Th}}^{\text{eff}} = \Phi + (1 - \Phi)D_{\text{Th}} \quad (44)$$

where mass porosity Φ is related to volume porosity ϕ by Eqn. 39. According to Eqns. 42–44, we obtain

$$F_{\text{Th}}/F_{\text{U}} = D_{\text{U}}^{\text{eff}}/D_{\text{Th}}^{\text{eff}} \quad (45)$$

Substituting Eqn. 45 into Eqn. 22 for the initial activity ratio, we have

$$(^{230}\text{Th})_f^0 / (^{238}\text{U})_f^0 = D_{\text{U}}^{\text{eff}}/D_{\text{Th}}^{\text{eff}} = \frac{\Phi + (1 - \Phi)D_{\text{U}}}{\Phi + (1 - \Phi)D_{\text{Th}}} \quad (46)$$

Consequently, the initial ratio ($^{230}\text{Th})_f^0 / (^{238}\text{U})_f^0$ is actually the inverse ratio of effective distribution coefficient of Th over that of U. According to Eqn. 46, the initial ratio when $f = \Phi$ is controlled by D_{U} , D_{Th} and Φ , and is independent of melting rate. As for another case when $f < \Phi$, melting takes place in a closed system, and the melting process is the same as batch melting (Figs. 1 and 3 in Zou, 1998). Replacing Φ in Eqn. 46 by f , we can obtain the equation for $f < \Phi$,

$$(^{230}\text{Th})_f / (^{238}\text{U})_f = \frac{f + (1-f)D_{\text{U}}}{f + (1-f)D_{\text{Th}}} \quad (47)$$

Therefore, when $f \leq \Phi$, ($^{230}\text{Th})_f / (^{238}\text{U})_f$ in the residual melt only depends on the bulk distribution coefficients of Th and U and the degree of melting (f), and is independent of melting rate, which is unlike the case when $f > \Phi$.

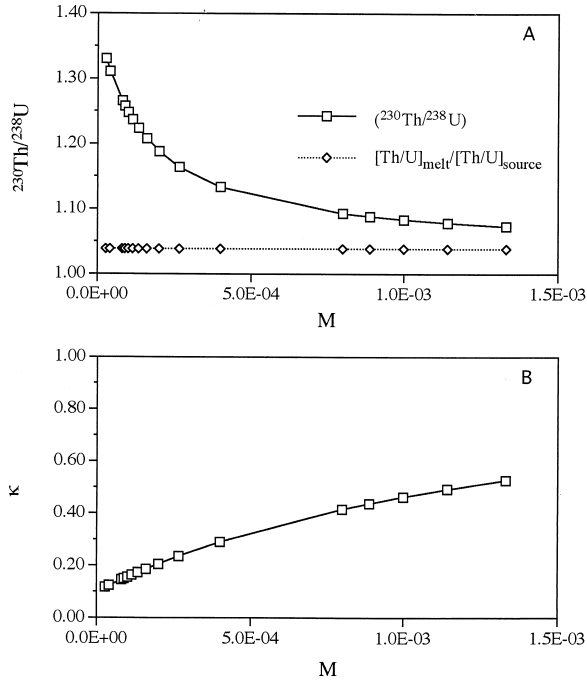


Fig. 3. (A) Variation of $(^{230}\text{Th}/^{238}\text{U})$ in the extracted melt as a function of \dot{M} for a fixed ϕ (0.3%) and X (2.4%) produced by melting of a garnet peridotite source. The value of $[\text{Th}/\text{U}]_{\text{melt}}/[\text{Th}/\text{U}]_{\text{source}}$ represents the Th/U ratio in the extracted melt normalized to its source Th/U ratio. $[\text{Th}/\text{U}]_{\text{melt}}/[\text{Th}/\text{U}]_{\text{source}}$ is calculated using Eqn. 21 for stable elements. The identical $[\text{Th}/\text{U}]_{\text{melt}}/[\text{Th}/\text{U}]_{\text{source}}$ can also be calculated using Eqns. 17 and 18 by setting λ of every nuclide to be zero. $(^{230}\text{Th}/^{238}\text{U})$ decreases as the melting rate increases, in contrast, $[\text{Th}/\text{U}]_{\text{melt}}/[\text{Th}/\text{U}]_{\text{source}}$ is independent of the rate of melting and is significantly smaller than $(^{230}\text{Th}/^{238}\text{U})$. (B) The relative contribution of net elemental U-Th fractionation to the total $^{230}\text{Th}/^{238}\text{U}$ disequilibrium as a function of melting rate for a fixed ϕ (0.3%) and X (2.4%). The bulk distribution coefficients for U and Th in Figure 3 are the same as those in Figure 1.

4.4. U-Series Modeling Vs. Trace Element Modeling

There is fundamental difference between trace element modeling and U-series modeling of the extracted melt. Melting rate affects U-series systematics but not stable element concentrations, as pointed out by O'Nions and McKenzie (1983) and Elliott (1997). Here we will explore this subject more quantitatively. According to Eqn. 21, trace element concentration in the extracted melt is a function of ϕ and X (or ϕ and f) and is independent of the melting rate (\dot{M}). In comparison, on the basis of Eqns. 17–19, the activities of U-series nuclides in the extracted melt depend on the rate of melting. Although ^{238}U and ^{235}U can be treated as stable nuclides for the time scale of melting because of their long half lives, we can not treat (^{230}Th) , (^{226}Ra) , and (^{231}Pa) the same way. This is due to the fact that, unlike ^{238}U and ^{235}U , the decay constants for ^{230}Th , ^{226}Ra and ^{231}Pa are too large to be ignored when compared with the melting parameter α (see, e.g., Eqns. 9–10 and 18–19). The difference between U-series modeling and trace element modeling can also be shown graphically. We take U-Th disequilibrium as an example. Figure 3A compares the relative extent of U/Th fractionation versus ingrowth as a function of

melting rate. It can be seen that, for a given fraction of extracted melt and a given porosity, $(^{230}\text{Th}/^{238}\text{U})$ strongly depends on the melting rate whereas the source-normalized Th/U concentration ratio, $[\text{Th}/\text{U}]_{\text{melt}}/[\text{Th}/\text{U}]_{\text{source}}$, is independent of the melting rate and is significantly lower than $(^{230}\text{Th}/^{238}\text{U})$. Figure 3A can also elucidate an important point that could be tied back into existing data sets. For example, Hawaiian basalts have a large buoyancy flux (i.e. upwelling rate) and little growth (Cohen and O'Nions, 1993; Sims et al., 1995) while MORBs have much lower upwelling rates and considerable ingrowth.

Both net elemental U-Th fractionation and ^{230}Th ingrowth contribute to the total U-Th disequilibrium. The total U-Th disequilibrium can be expressed as $(^{230}\text{Th}/^{238}\text{U}) - 1$, where $(^{230}\text{Th}/^{238}\text{U})$ is calculated from Eqn. 27. Net elemental U-Th fractionation can be expressed as $[\text{Th}/\text{U}]_{\text{melt}}/[\text{Th}/\text{U}]_{\text{source}} - 1$, where $[\text{Th}/\text{U}]_{\text{melt}}/[\text{Th}/\text{U}]_{\text{source}}$ can be calculated from Eqn. 21. Consequently, the ^{230}Th ingrowth can be expressed as $(^{230}\text{Th}/^{238}\text{U}) - [\text{Th}/\text{U}]_{\text{melt}}/[\text{Th}/\text{U}]_{\text{source}}$. The relative contribution from net elemental U-Th fractionation to the total U-Th disequilibrium can be quantified as

$$\kappa = \frac{[\text{Th}/\text{U}]_{\text{melt}}/[\text{Th}/\text{U}]_{\text{source}} - 1}{(^{230}\text{Th}/^{238}\text{U}) - 1} \quad (48)$$

The relative contribution of ^{230}Th ingrowth to total U-Th disequilibrium is thus

$$1 - \kappa = \frac{(^{230}\text{Th}/^{238}\text{U}) - [\text{Th}/\text{U}]_{\text{melt}}/[\text{Th}/\text{U}]_{\text{source}}}{(^{230}\text{Th}/^{238}\text{U}) - 1} \quad (49)$$

κ strongly depends on the melting rate and its magnitude is usually significantly less than 1 (Fig. 3B). Net elemental fractionation is significant only when the melting rate is large. It should be pointed out that κ is also strongly dependent on the decay constant of the daughter nuclide. The larger its decay constant (i.e., the shorter its half life), the smaller the κ . This is part of the reason why Th-Ra and U-Pa disequilibria are more noted than U-Th disequilibrium in young lavas. Since κ is usually significantly less than 1, we can not use the equations for trace element fractionation to model (^{230}Th) , (^{226}Ra) , (^{231}Pa) , $(^{230}\text{Th}/^{238}\text{U})$, $(^{226}\text{Ra}/^{230}\text{U})$, or $(^{231}\text{Pa}/^{235}\text{U})$ by assuming that net elemental fractionation alone is responsible for the U-series disequilibria. Otherwise, the inferred degree of partial melting to produce basalts would be unrealistically too small.

In summary, this paper provides the equations for modeling of U-series disequilibria during mantle dynamic melting and evaluates the effects of melting porosity, melting rate, melting time and distribution coefficients on U-series disequilibria. The physical concepts of melting rate and melting time are clarified and quantitatively defined. U-series modeling is quantitatively compared with trace element modeling. Trace element fractionation is independent of melting rate, in contrast, melting rate plays an important role in U-series disequilibria. Both net elemental fractionation and ingrowth of daughter nuclides contribute to the total U-series disequilibria. The ingrowth of daughter nuclides is dominant when the melting rate is slow and when the half-life of the daughter nuclide is short. Since U-series disequilibria can not be attributed to net elemental fractionation alone, one cannot use the equations for trace

element fractionation to model U-series disequilibria in young lavas produced by mantle melting.

Acknowledgments—We are very grateful to Tim Elliott and Ken Sims for their constructive journal reviews that considerably improved the quality of the paper. Vincent Salters, David Loper, and Roy Odom provided useful comments. We also thank Karl Turekian for his handling of this manuscript. This work was in part supported by a National Science Foundation Earth Sciences Postdoctoral Research Fellowship Award to HZ and an NSF grant to AZ.

REFERENCES

- Allègre C. J. and Condomines M. (1982) Basalt genesis and mantle structure studied through Th-isotopic geochemistry. *Nature* **299**, 21–24.
- Beattie P. (1993a) Uranium-thorium disequilibria and partitioning on melting of garnet peridotite. *Nature* **363**, 63–65.
- Beattie P. (1993b) The generation of uranium series disequilibria by partial melting of spinel peridotite: Constraints from partitioning studies. *Earth Planet. Sci. Lett.* **117**, 379–391.
- Bourdon B., Langmuir C. H., and Zindler A. (1996) Ridge-hotspot interaction along the Mid-Atlantic ridge between 37°30' and 40°30'N: The U-Th disequilibrium evidence. *Earth Planet. Sci. Lett.* **142**, 175–189.
- Chabaux F. and Allègre C. J. (1994) ^{238}U - ^{230}Th - ^{226}Ra disequilibria in volcanics: A new insight into melting conditions. *Earth Planet. Sci. Lett.* **126**, 61–74.
- Cohen A. S. and O'Nions R. K. (1993) Melting rates beneath Hawaii: Evidence from uranium series isotopes in recent lavas. *Earth Planet. Sci. Lett.* **120**, 169–175.
- Elliott T. (1997) Fractionation of U and Th during mantle melting: A reprise. *Chem. Geol.* **139**, 165–183.
- Hauri E. H., Wagner T. P., and Grove T. L. (1994) Experimental and natural partitioning of Th, U, Pb and other trace elements between garnet, clinopyroxene and basaltic melts. *Chem. Geol.* **117**, 149–166.
- Hemond C., Hofmann A. W., Heusser G., Condomines M., Raczek I., and Rhodes J. M. (1994) U-Th-Ra systematics in Kilauea and Mauna Loa basalts, Hawaii. *Chem. Geol.* **116**, 163–180.
- Iwamori H. (1994) ^{238}U - ^{230}Th - ^{226}Ra and ^{235}U - ^{231}Pa disequilibria produced by mantle melting with porous and channel flows. *Earth Planet. Sci. Lett.* **125**, 1–16.
- Johnson K. T. M., Dick H. J. B., and Shimizu N. (1990) Melting in the oceanic mantle: An ion microprobe study of diopside in abyssal peridotite. *J. Geophys. Res.* **95**, 2661–2678.
- LaTourrette T. Z. and Burnett D. S. (1992) Experimental determination of U and Th partitioning between clinopyroxene and natural and synthetic basaltic liquid. *Earth Planet. Sci. Lett.* **110**, 227–244.
- LaTourrette T. Z., Kennedy A. K., and Wasserburg G. J. (1993) Thorium-uranium fractionation by garnet: Evidence for a deep source and rapid rise of oceanic basalts. *Sciences* **261**, 739–742.
- Lundstrom C. C., Shaw H. F., Ryerson F. J., Phinney D. L., Gill J. B., and Williams Q. (1994) Compositional controls on the partitioning of U, Th, Ba, Pb, Sr, and Zr between clinopyroxene and haplobasaltic melts: Implications for uranium series disequilibria in basalts. *Earth Planet. Sci. Lett.* **128**, 407–423.
- Lundstrom C. C., Gill J., Williams Q., and Perfit M. R. (1995) Mantle melting and basalt extraction by equilibrium porous flow. *Science* **270**, 1958–1961.
- McKenzie D. (1985) The extraction of magma from the crust and mantle. *Earth Planet. Sci. Lett.* **74**, 81–91.
- McKenzie D. (1985) ^{230}Th - ^{238}U disequilibrium and the melting processes beneath ridge axes. *Earth Planet. Sci. Lett.* **72**, 149–157.
- Pickett D. A. and Murrell M. T. (1997) Observation of 231Pa/235U disequilibrium in volcanic rocks. *Earth Planet. Sci. Lett.* **148**, 259–271.
- O'Nions R. K. and McKenzie D. (1993) Estimates of mantle thorium/uranium ratios from Th, U and Pb isotope abundances in basaltic melts. *Phil. Trans. R. Soc. Lond. A.* **342**, 65–77.
- Qin Z. (1993) Dynamics of melt generation beneath mid-ocean ridge axes: Theoretical analysis based on ^{238}U - ^{230}Th - ^{226}Ra and ^{235}U - ^{231}Pa disequilibria. *Geochim. Cosmochim. Acta* **57**, 1629–1634.
- Richardson C. and McKenzie D. (1994) Radioactive disequilibria from 2D models of melt generation by plumes and ridges. *Earth Planet. Sci. Lett.* **128**, 425–437.
- Rubin K. H. and Macdougall J. D. (1988) ^{226}Ra excesses in mid-ocean ridge basalts and mantle melting. *Nature* **335**, 158–161.
- Salters V. J. M. and Longhi J. (1999) Trace element partitioning during the initial stages of melting beneath mid-ocean ridges. *Earth Planet. Sci. Lett.* **166**, 15–30.
- Sims K. W. W., DePaolo D. J., Murrell M. T., Baldrige W. S., Goldstein S. J., and Clague D. A. (1995) Mechanisms of magma generation beneath Hawaii and mid-ocean ridges: Uranium/thorium and samarium/neodymium isotopic evidence. *Science* **267**, 508–512.
- Spiegelman M. and Elliott T. (1993) Consequences of melt transport for uranium series disequilibrium in young lavas. *Earth Planet. Sci. Lett.* **118**, 1–20.
- Williams R. W. and Gill J. B. (1989) Effect of partial melting on the uranium decay series. *Geochim. Cosmochim. Acta* **53**, 1607–1619.
- Wood B. J., Blundy J. D., and Robinson J. A. C. (1999) The role of clinopyroxene in generating U-series disequilibrium during mantle melting. *Geochim. Cosmochim. Acta* **63**, 1613–1620.
- Zou H. (1998) Trace element fractionation during modal and nonmodal dynamic melting and open-system melting: A mathematical treatment. *Geochim. Cosmochim. Acta* **62**, 1937–1945.